Dalton Transactions

Cite this: *Dalton Trans.*, 2011, **40**, 12584

www.rsc.org/dalton

**PAPER**

# The intramolecular aryl embrace: from light emission to light absorption†

**Biljana Bozic-Weber, Edwin C. Constable,* Catherine E. Housecroft,* Peter Kopecky, Markus Neuburger and Jennifer A. Zampese**

***Received 6th June 2011, Accepted 2nd September 2011***
**DOI: 10.1039/c1dt11052g**



6-(1-Methylpyrrol-2-yl)-2,2′-bipyridine, **3**, and 6-(selenophene-2-yl)-2,2′-bipyridine, **4**, have been prepared and characterized in solution and by structural determinations. Copper(I) complexes $[CuL_2][PF_6]$ in which L is 2,2′-bipyridine substituted in the 6-position by furyl, thienyl, *N*-methylpyrrolyl, selenopheneyl, methyl or phenyl, (L = **1–6**) have been synthesized. The complexes have been characterized by electrospray mass spectrometry, and solution NMR and UV-VIS spectroscopies. The single crystal structures of $[Cu(\mathbf{1})_2][PF_6]$, $[Cu(\mathbf{2})_2][PF_6]$, $[Cu(\mathbf{3})_2][PF_6]$, $[Cu(\mathbf{5})_2][PF_6]$ and $[Cu(\mathbf{6})_2][PF_6]$ have been determined. In those compounds containing an aromatic substituent attached to the bpy unit, the substituent is twisted with respect to the latter. In $[Cu(\mathbf{3})_2][PF_6]$ and $[Cu(\mathbf{5})_2][PF_6]$, this results in intra-cation π-stacking between ligands which is very efficient in $[Cu(\mathbf{3})_2]^+$ despite the steric requirements of the *N*-methyl substituents. Face-to-face stacking between the ligands in the $[Cu(\mathbf{2})_2]^+$ ion is achieved by complementary substituent twisting and elongation of one Cu–N bond, but there is no analogous intra-cation π-stacking in $[Cu(\mathbf{1})_2]^+$. Ligand exchange reactions between $[CuL_2][PF_6]$ (L = **1–6**) and $TiO_2$-anchored ligands **7–10** (L′ = 2,2′-bipyridine-based ligands with $CO_2H$ or $PO(OH)_2$ anchoring groups) have been applied to produce 24 surface-anchored heteroleptic copper(I) complexes, the formation of which has been evidenced by using MALDI-TOF mass spectrometry and thin layer solid state diffuse reflectance electronic absorption spectroscopy. The efficiencies of the complexes as dyes in DSCs have been measured, and the best efficiencies are observed for [CuLL′] with L′ = **10** which contains phosphonate anchoring groups.

## Introduction

As part of our ongoing interest in Earth-abundant metals for applications in dye-sensitized solar cells (DSCs), we are investigating a broad variety of copper(I) complexes. To date, there have been only a few literature reports of copper(I)-based DSCs.[1–9] Our past efforts have focused on incorporating ligands functionalized with substituents such as carboxylates to anchor the complex to a $TiO_2$ surface.[4,9,10] Copper(I) complexes are labile[11,12] and this property has been successfully applied for establishing dynamic libraries,[13–15] and for preparing heteroleptic copper(I) complexes.[16–18] In a preliminary report,[6] we showed that oligopyridine ligands undergo rapid exchange at copper(I). This forms the basis of a new strategy for the assembly of copper(I) complexes directly on a semiconductor surface: initial binding of an oligopyridine ligand, L′, containing anchoring groups onto the surface, followed by introduction of a $[CuL_2]^+$ complex which undergoes ligand exchange to give a surface-bound heteroleptic $[CuLL']^+$ complex. This methodology should enable efficient screening of families of complexes without the need for isolation of the heteroleptic species. Although the photophysical properties of copper(I) oligopyridine complexes have been intensively studied and are known to be critically dependent upon ligand substitution[19] little is known about the influence on their effectiveness as photosensitisers. On the other hand, in the context of complexes in light emitting electrochemical cells, we have shown that intramolecular stabilization of cations by face-to-face π-stacking of aromatic substituents at the 6-position of 2,2′-bipyridines (an "aryl embrace") leads to enhanced device performance.[20] The enhancement of the emission behaviour in copper(I) bis(1,10-phenanthroline) complexes by the incorporation of appropiate substituents has been demonstrated by McMillin and coworkers.[21] In this paper, we extend our studies to the use of 6-aryl-2,2′-bipyridines in DSCs and describe the synthesis and characterization of a series of homoleptic $[CuL_2]^+$ complexes in which L is a 2,2′-bipyridine ligand, substituted in the 6-position by methyl, phenyl or an aromatic heterocycle (L = **1–6**, Scheme 1). We have then subjected these complexes to exchange reactions on a $TiO_2$ surface and assessed the performance of the resulting heteroleptic complexes in DSCs. Although we present solid-state structural data for the

*Department of Chemistry, University of Basel, Spitalstrassse 51, CH-4056, Basel, Switzerland. E-mail: catherine.housecroft@unibas.ch, edwin.constable@unibas.ch; Fax: +41 61 267 1018; Tel: +41 61 267 1008*

† Electronic supplementary information (ESI) available: Fig. S1–S5 show thin layer solid state diffuse reflectance electronic absorption spectra of $TiO_2$-anchored ligands **7–10** after treatment with $[CuL_2][PF_6]$ (L = **1**, **2**, **4–6**). CCDC reference numbers 828945–828951. For ESI and crystallographic data in CIF or other electronic format see DOI: 10.1039/c1dt11052g

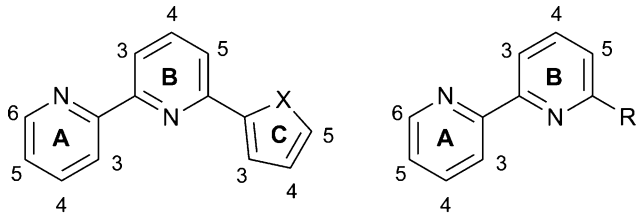


**Scheme 1** Ligand structures and labelling for $^{1}$H NMR spectroscopic assignments.

homoleptic complexes, it is important to remember that the precise geometries of the complexes in the films in the DSCs are unknown and most unlikely to be microscopically identical to those in the solid state. The choice of the heterocyclic substituents in this study follows from the known ability of thiophene to tune the electronic properties of 2,2′-bipyridine.[22] Although the chemistry of 6-(2-thienyl)-2,2′-bipyridine, **2**, has been explored to some extent, that of analogous ligand **1** has been little studied, while derivatives **3** and **4** have not, to the best of our knowledge, been reported. We note that **2** exhibits a versatile coordination chemistry in its reactions with ruthenium(II), ruthenium(III), palladium(II), platinum(II) and gold(III).[23–30]

## Experimental

Infrared spectra were recorded on a Shimadzu FTIR 8400 S Fourier-transform spectrophotometer with solid samples with a Golden Gate ATR. $^{1}$H and $^{13}$C NMR spectra were recorded on Bruker AM 400 or DRX 500 spectrometers; chemical shifts are with respect to residual solvent peaks (TMS $\delta$ 0 ppm). $^{77}$Se NMR spectra were recorded on a Bruker Avance III NMR spectrometer operating 600.13 MHz proton frequency; the instrument is equipped with a 5-mm broadband direct observe probe (BBFO+); $^{77}$Se chemical shifts were referenced externally, relative to selenophene in $CD_2Cl_2$ at a shift of 605 ppm. Solution UV/VIS spectroscopic measurements were recorded using a Varian Cary 5000 spectrophotometer. Solid state diffuse reflectance electronic absorption spectra of Cu(I)-containing dyes on $TiO_2$ were measured using a Varian Cary 5000 with diffuse reflectance accessory and a conducting glass with a $TiO_2$ layer as a blank. Emission spectra were recorded on Shimadzu 5301PC spectrofluorophotometer. EI and electrospray (ESI) mass spectra were recorded on Finnigan MAT 95, Finnigan MAT LCT or LCQ mass spectrometers, and MALDI-TOF mass spectra with a PerSeptive Biosystems Voyager instrument.

Ligand **1** was prepared by Kröhnke methodology[31,32] as previously reported. $[Cu(NCMe)_4][PF_6]$ was prepared by the literature method.[33] Ligands **5** and **6** were made following literature procedures.[34]

### Compound 2: method 1

$^{n}$BuLi (1.6 M in hexanes, 11 mmol, 6.3 ml) was added to a solution of thiophene (0.80 ml, 10.0 mmol) in THF (20 ml) at 223–233 K. The yellow solution was stirred for ≈1 h, after which time bpy (1.56 g, 10.0 mmol) was added. The reaction mixture turned red immediately. The suspension was allowed to warm to room temperature and was then stirred for 12 h. After quenching the reaction with $H_2O$, the organic layer was separated and the aqueous phase extracted 3 times with $CH_2Cl_2$. The organic layers were combined and an excess of $MnO_2$ was added. The black suspension was stirred at room temperature overnight and was then dried over $MgSO_4$. The solids were separated by filtration, the solvent removed *in vacuo*, and the product purified by column chromatography (silica M60, $CH_2Cl_2$ changing to $CH_2Cl_2$/MeOH 99 : 1–97 : 3). Compound **2** was obtained as a brown oil as the 1st major fraction, and after recrystallization from hexanes, **2** was isolated as white crystals (220 mg, 10%). The 2nd major fraction was identified as 4-(thiophen-2-yl)-2,2′-bipyridine[35] (260 mg, 12%). Spectroscopic data for **2** were in agreement with those published.[23,35]

### Compound 2: method 2

2-Acetylthiophene (1.26 g, 10 mmol) was added to a solution of KO$^{t}$Bu (2.24 g, 20 mmol) in dry THF (30 ml). The mixture was stirred for 2 h at room temperature during which time it turned yellow. 1-(Pyridin-2-yl)-3-*N*,*N*-dimethylamino-prop-2-en-1-one[36–38] (1.76 g, 10 mmol) was added and the reaction mixture was stirred for 14 h during which time it became deep red. Excess solid $NH_4OAc$ and HOAc (25 ml) were added and the mixture was stirred under reflux for 2 h to give a black solution. The solvents were removed *in vacuo* and the black residue was suspended in $H_2O$ and the pH adjusted to 8 by adding solid $K_2CO_3$. The aqueous phase was extracted several times with $CH_2Cl_2$, the organic phases were combined and dried over $MgSO_4$. After removing the solvent under reduced pressure, the resulting black oil was dissolved in toluene and filtered through Celite. The solvent was evaporated to give a brown paste which was passed through a column ($SiO_2$ 60 μ, 18 cm, hexanes/EtOAc) to give two products, 2,6-bis(thiophen-2-yl)-pyridine[39] as the 1st major fraction (245 mg, 10% or 20% relative to 2-acetylthiophene, respectively) and compound **2** as the 2nd major fraction (430 mg, 18%). Spectroscopic data for **2** were in agreement with those published.[23,35]

### Compound 3

1-Methylpyrrole (2.03 g, 25.0 mmol) was added to dry THF (20 ml) and the solution was cooled to 223 K. $^{n}$BuLi (18.8 ml, 1.6 M) was added and the reaction mixture was stirred for 1 h and then warmed to 273 K. 2,2′-Bipyridine (3.51 g, 22.5 mmol) was added and the red suspension was allowed to warm to room temperature after which it was stirred for 12 h. The reaction mixture was quenched with water and the organic layer removed. The aqueous layer was extracted three times with $CH_2Cl_2$. An excess of $MnO_2$ was added to the combined $CH_2Cl_2$ layers and the resulting black suspension was stirred at room temperature overnight. After drying over $MgSO_4$, the mixture was filtered and the filtrate collected. Solvent was removed *in vacuo*, and the product purified by coloumn chromatography (silica M60, pentane/ethyl acetate 95 : 5 changing to 9 : 1). **3** was isolated as a white crystalline solid (0.907 g, 15.4%). $^{1}$H NMR (500 MHz, $CD_2Cl_2$) $\delta$ (ppm) 8.67 (dd, $J$ = 4.7, 0.7 Hz, 1H, $H^{A6}$), 8.44 (d, $J$ = 7.9 Hz, 1H, $H^{A3}$), 8.24 (d, $J$ = 7.8 Hz, 1H, $H^{B3}$), 7.84 (t, $J$ = 7.7 Hz,

1H, $H^{A4}$), 7.79 (t, $J$ = 7.8 Hz, 1H, $H^{B4}$), 7.59 (d, $J$ = 7.8, 1H, $H^{B5}$), 7.32 (m, 1H, $H^{A5}$), 6.79 (m, 1H, $H^{C5}$), 6.65 (m, 1H, $H^{C3}$), 6.18 (t, $J$ = 3.2 Hz, 1H, $H^{C4}$), 4.13 (s, 3H, $H^{Me}$); $^{13}C\{^1H\}$ NMR (126 MHz, $CD_2Cl_2$) $\delta$ (ppm) 156.9 ($C^{A2}$), 155.4 ($C^{B2}$), 152.6 ($C^{B6}$), 149.6 ($C^{A6}$), 137.8 ($C^{B4}$), 137.4 ($C^{A4}$), 132.2 ($C^{C2}$), 127.0 ($C^{C5}$), 124.2 ($C^{A5}$), 121.8 ($C^{B5}$), 121.3 ($C^{A3}$), 117.9 ($C^{B3}$), 111.4 ($C^{C3}$), 108.1 ($C^{C4}$), 37.9 ($C^{Me}$); IR (solid, $\nu$/cm$^{-1}$) 2964 (w), 2937 (w), 2358 (w), 2331 (w), 1580 (m), 1566 (m), 1556 (m), 1456 (m), 1435 (m), 1157 (w), 1097 (w), 775 (w), 721 (w), 530 (s); UV/VIS ($CH_2Cl_2$, $1.0 \times 10^{-5}$ mol dm$^{-3}$) $\lambda_{max}$/nm 237 ($\varepsilon$/dm$^3$ mol$^{-1}$ cm$^{-1}$ 18 300), 281 (18 700), 303 (17 000); emission ($\lambda_{ex}$ = 282 nm) $\lambda_{em}$ = 457 nm; EI MS: $m/z$ 235.1 $[M]^+$ (calc. 235.1), 234.1 $[M - H]^+$ (base peak, calc. 234.1). Found C 76.54, H 5.64, N 17.88; $C_{15}H_{13}N_3$ requires C 76.57, H 5.57, N 17.86%.

### Compound 4

$^n$BuLi (1.6 M in hexanes, 1.6 ml, 2.6 mmol) was added to a solution of selenophene (190 µl, 2.2 mmol) in THF (12 ml) at 190 K. The pale yellow solution was stirred for 1 h, after which bpy (310 mg, 2.0 mmol) was added. The reaction mixture slowly turned red. The suspension was allowed to warm to room temperature and then was stirred for 12 h during which time it became deep red. After quenching the reaction with $H_2O$, the organic layer was separated and the aqueous phase was extracted 3 times with $CH_2Cl_2$. The organic layers were combined and an excess of $MnO_2$ was added. The black suspension was stirred at room temperature overnight, and dried over $MgSO_4$. The precipitate was removed by filtration and the filtrate collected. After solvent removal *in vacuo*, the product was purified by column chromatography (silica M60, pentane/ethylacetate 95 : 5 to 9: 1). Compound **4** was isolated as an yellow solid (160 mg, 28%). $^1H$ NMR (500 MHz, $CD_2Cl_2$) $\delta$ (ppm) 8.67 (d, $J$ = 4.1 Hz, 1H, $H^{A6}$), 8.51 (d, $J$ = 7.9 Hz, 1H, $H^{A3}$), 8.31 (d, $J$ = 7.8 Hz, 1H, $H^{B3}$), 8.10 (d, $J$ = 5.6 Hz, 1H, $H^{C5}$), 7.87 (t, $J$ 7.7 Hz, 1H, $H^{A4}$), 7.83 (m, 2H, $H^{B4+C3}$), 7.72 (d, $J$ = 7.8 Hz, 1H, $H^{B5}$), 7.41 (m, 1H, $H^{C4}$), 7.34 (m, 1H, $H^{A5}$); $^{13}C\{^1H\}$ NMR (101 MHz, $CD_2Cl_2$) $\delta$ 156.2 ($C^{A2/B2}$), 156.1 ($C^{A2/B2}$), 153.7 ($C^{C2}$), 152.7 ($C^{B6}$), 149.6 ($C^{A6}$), 138.2 ($C^{B4}$), 137.5 ($C^{A4}$), 133.4 ($C^{C5}$), 131.4 ($C^{C4}$), 126.7 ($C^{C3}$), 124.5 ($C^{A5}$), 121.5 ($C^{A3}$), 119.7 ($C^{B3}$), 118.1 ($C^{B5}$); $^{77}Se\{^1H\}$ NMR (114 MHz, $CD_2Cl_2$) $\delta$ (ppm) 603.1; IR (solid, $\nu$/cm$^{-1}$) 3049 w, 2922 w, 2851 w, 1580 w, 1562 s, 1541 w, 1454 w, 1423 s, 1265 (w), 1225 w, 1151 w, 1092 w, 1078 w, 1045 w, 989 w, 968 w, 912 w, 847 w, 824 w, 771 s, 735 s, 704 s, 677 s, 648 w. UV/VIS ($CH_2Cl_2$, $1.0 \times 10^{-5}$ mol dm$^{-3}$) $\lambda_{max}$/nm 241 ($\varepsilon$/dm$^3$ mol$^{-1}$ cm$^{-1}$ 11 500), 275 (13 500), 312 (11 000). ESI MS: $m/z$ 309.0 $[M + Na]^+$ (base peak, calc. 309.0), 287.3 $[M + H]^+$ (calc. 287.0). Found C 58.89, H 3.57, N 9.68; $C_{14}H_{10}N_2Se$ requires C 58.96, H 3.53, N 9.82%.

### Copper complexes: general method

Each synthesis was carried out on an 50 µmol scale unless otherwise stated. $[Cu(NCMe)_4][PF_6]$ (18.6 mg, 50 µmol) was dissolved in MeCN and the ligand (100 µmol) was added. The solution turned deep red immediately. It was stirred for 2 h with TLC monitoring until all free ligand has been consumed. Solvent was removed *in vacuo*, leaving a red or black residue. The product was recrystallized from EtOH when necessary.

### $[Cu(1)_2][PF_6]$

$[Cu(\mathbf{1})_2][PF_6]$ was isolated as red crystals (28 mg, 95%). $^1H$ NMR (500 MHz, $CD_2Cl_2$) $\delta$ (ppm) 8.32 (br, 4H, $H^{A3+B3}$), 8.15 (br, 2H, $H^{A6}$), 8.07 (br, 4H, $H^{A4+B4}$), 7.86 (br, 2H, $H^{B5}$), 7.51 (br, 2H, $H^{A5}$), 7.07 (br, 2H, $H^{C5}$), 6.85 (br, 4H, $H^{C3}$), 6.05 (br, 2H, $H^{C4}$); IR (solid, $\nu$/cm$^{-1}$) 3159w, 3132w, 2961w, 2932w, 2868w, 2361w, 2326w, 1981w, 1724w, 1599w, 1558w, 1497w, 1474w, 1452w, 1439w, 1412w, 1321w, 1298w, 1275w) 1248w, 1223w, 1165w, 1101w, 1074w, 1011w, 995w, 914w, 881w, 849 s, 825 s, 762 s, 744 s, 731w, 690w, 675w. UV/VIS ($CH_2Cl_2$, $1.0 \times 10^{-5}$ mol dm$^{-3}$) $\lambda_{max}$/nm 240 ($\varepsilon$/dm$^3$ mol$^{-1}$ cm$^{-1}$ 26 300), 275 (21 100), 300 (19 000), 328 (23 800), 420 (2600), 520 (1900). ESI MS: $m/z$ 507.1 $[M - PF_6]^+$ (base peak, calc. 507.1). Found: C 52.30, H 3.08, N 8.39; $C_{28}H_{20}CuF_6N_4O_2P$ requires C 51.50, H 3.09, N 8.58%.

### $[Cu(2)_2][PF_6]$

$[Cu(\mathbf{2})_2][PF_6]$ was isolated as red crystals (33 mg, 97%). $^1H$ NMR (500 MHz, $CD_2Cl_2$) $\delta$ (ppm) 8.32 (br, 2H, $H^{A3}$), 8.22 (br, 2H, $H^{A6}$), 8.05 (br, 4H, $H^{A4+B3}$), 7.94 (br, 2H, $H^{B4}$), 7.61 (br, 2H, $H^{B5}$), 7.51 (br, 2H, $H^{A5}$), 7.27 (br, 2H, $H^{C5}$), 6.99 (br, 2H, $H^{C3}$), 6.61 (br, 2H, $H^{C4}$). IR (solid, $\nu$/cm$^{-1}$) 3109w, 2348w, 1669w, 1593 m, 1558 m, 1526w, 1480w, 1447 s, 1423 m, 1394 m, 1353w, 1258 m, 1228 m, 1177 m, 1162 m, 1120 w, 1092 w, 1057 w, 1002 w, 825 s, 814 s, 770 s, 740 s, 702 s, 690 s, 655 m, 633 m; UV/VIS ($CH_2Cl_2$, $2.1 \times 10^{-5}$ mol dm$^{-3}$) $\lambda_{max}$/nm 242 ($\varepsilon$/dm$^3$ mol$^{-1}$ cm$^{-1}$ 32 400), 270 (22 600), 320 (22 400), 410 (2500), 530 (1600). ESI MS: $m/z$ 539.0 $[M - PF_6]^+$ (base peak, calc. 539.0). Found: C 49.12, H 2.99, N 7.90; $C_{28}H_{20}CuF_6N_4PS_2$ requires C 49.09, H 2.94, N 8.18%.

### $[Cu(3)_2][PF_6]$

The synthesis was carried out on a 213 µmol scale. $[Cu(\mathbf{3})_2][PF_6]$ was isolated as red crystals (107 mg, 74%). $^1H$ NMR (500 MHz, $CD_2Cl_2$) $\delta$ (ppm) 8.61 (br, 2H, $H^{A6}$), 8.15 (br, 2H, $H^{B4}$), 8.08 (br, 2H, $H^{A4}$), 7.91 (br, 4H, $H^{A3+B3}$), 7.61 (br, 2H, $H^{A5}$), 7.41 (br, 2H, $H^{B5}$), 6.10 (br, 2H, $H^{C5}$), 5.76 (br, 2H, $H^{C3}$), 5.55 (br, 2H, $H^{C4}$), 3.28 (s, 6H, $H^{Me}$); $^{13}C\{^1H\}$ NMR (126 MHz, $CD_2Cl_2$) $\delta$ (ppm) 153.3 ($C^{A2}$), 152.7 ($C^{B2}$), 150.8 ($C^{B6}$), 149.0 ($C^{A6}$), 138.2 ($C^{A4}$), 132.3 ($C^{C2}$), 126.6 ($C^{A5+B5}$), 125.3 ($C^{C5}$), 122.7 ($C^{C4}$), 120.3 ($C^{A3+B3}$), 111.4 ($C^{C3}$), 108.3 ($C^{C4}$), 35.2 ($C^{Me}$). IR (solid, $\nu$/cm$^{-1}$) 3124 w, 3090 w, 2939 w, 2919 w, 2360 w, 2331 w, 1988 w, 1663 m, 1599 m, 1569 m, 1558 m, 1487 m, 1456 s, 1444 s, 1423 m, 1390 m, 1321 m, 1299 m, 1248 m, 1222w, 1177 m, 1157 m, 1090 m, 1066 m, 1053 m, 1004 m, 990 w, 914 m, 893 m, 835 s, 833 s, 820 s, 800 s, 770 s, 745 s, 719 s, 678 m, 624 m; UV/VIS ($CH_2Cl_2$, $5.0 \times 10^{-5}$ mol dm$^{-3}$) $\lambda_{max}$/nm 242 ($\varepsilon$/dm$^3$ mol$^{-1}$ cm$^{-1}$ 27 700), 268 (29 700), 297 (27000), sh 330 (17 000), 430 (3200), 530 (1800). ESI MS $m/z$ 533.0 $[M - PF_6]^+$ (base peak, calc. 533.2). Found C 52.13, H 4.01, N 12.44; $C_{30}H_{26}CuF_6N_6P$ requires C 53.06, H 3.86, N 12.38%.

### $[Cu(4)_2][PF_6]$

$[Cu(\mathbf{4})_2][PF_6]$ was isolated as red crystals (37 mg, 95%). $^1H$ NMR (500 MHz, $CD_2Cl_2$) $\delta$ (ppm) 8.30 (br, 2H, $H^{A6}$), 8.23 (br, 2H, $H^{B4}$), 8.06 (br, 2H, $H^{A3+B3}$), 7.99 (br, 2H, $H^{A4}$), 7.76 (br, 2H, $H^{C5}$), 7.67 (br, 2H, $H^{B5}$), 7.48 (br, 4H, $H^{C3+A5}$), 6.92 (br, 2H, $H^{C4}$). IR (solid, $\nu$/cm$^{-1}$) 3115 w, 3101 w, 2926 w, 2854 w, 2361 w, 2338 w, 1724 w, 1653 w, 1593 w, 1558 w, 1539 w, 1481 w, 1448 s, 1433 w, 1394 w, 1340 w, 1294 w, 1258 w, 1225 w, 1178 w, 1161 w, 1121 w, 1078 w, 1053 w, 1016 w, 999 w, 972 w, 827 s, 768 w, 741 w, 692 w, 677 w, 654 w, 608 w. UV/VIS ($CH_2Cl_2$, $1.0 \times 10^{-5}$ mol dm$^{-3}$) $\lambda_{max}$/nm 247 ($\varepsilon$/dm$^3$ mol$^{-1}$ cm$^{-1}$ 29 000), 273 (25 300), 322 (22 200),

413 (3100), 531 (2300). ESI MS: *m/z* 635.0 $[M - PF_6]^+$ (base peak, calc. 634.9). Found: C 43.37, H 2.73, N 6.88, $C_{28}H_{20}CuF_6N_4PSe_2$ requires C 43.18, H 2.59, N 7.19%.

### [Cu(5)$_2$][PF$_6$]

[Cu(**5**)$_2$][PF$_6$] was isolated as red crystals (30 mg, 89%). $^1$H NMR (500 MHz, $CD_2Cl_2$) $\delta$ (ppm) 8.53 (d, $J$ = 4.7 Hz, 2H, $H^{A6}$), 8.16 (d, $J$ = 8.1 Hz, 2H, $H^{A3}$), 8.08 (t, $J$ = 7.7 Hz, 2H, $H^{A4}$), 7.92 (m, $J$ = 4.5 Hz, 4H, $H^{B3+B5}$), 7.57 (m, 2H, $H^{A5}$), 7.52 (m, 2H, $H^{B4}$), 7.29 (d, $J$ = 7.5 Hz, 4H, $H^{C2}$), 7.02 (t, $J$ = 7.4 Hz, 2H, $H^{C4}$), 6.80 (t, $J$ = 7.6 Hz, 4H, $H^{C3}$); $^{13}$C{$^1$H} NMR (126 MHz, $CD_2Cl_2$) $\delta$ (ppm) 158.2 ($C^{B6}$), 152.8 ($C^{A2/B2}$), 152.6 ($C^{A2/B2}$), 148.9 ($C^{A6}$), 139.5 ($C^{C1}$), 138.7 ($C^{B5}$), 138.4 ($C^{A4}$), 129.6 ($C^{C4}$), 128.1 ($C^{C3}$), 127.8 ($C^{C2}$), 126.8 ($C^{A5}$), 125.4 ($C^{B4}$), 122.8 ($C^{A3}$), 120.7 ($C^{B3}$); IR (solid, $\nu$/cm$^{-1}$) 3055 w, 2959 w, 2926 w, 2868 w, 2366 w, 2326 w, 1724 w, 1595 w, 1570 w, 1558 w, 1477 w, 1445 s, 1391 w, 1288 w, 1277 w, 1240 w, 1184 w, 1161 w, 1122 w, 1076 w, 1043 w, 1014 w) 1003 w, 928 w, 903 w, 878 w, 831 s, 814 s, 779 s, 754 s, 741 s, 698 s, 636 w. UV/VIS ($CH_2Cl_2$, $1.0 \times 10^{-5}$ mol dm$^{-3}$) $\lambda_{max}$/nm 232 ($\varepsilon$/dm$^3$ mol$^{-1}$ cm$^{-1}$ 38 100), 263 (28 500), 308 (26 200), 419 (4400), 526 (3000). ESI MS: *m/z* 527.2 $[M - PF_6]^+$ (base peak, calc. 527.1). Found C 57.22, H 3.95, N 7.41; $C_{32}H_{24}CuF_6N_4P$·EtOH requires C 56.79, H 4.20, N 7.79%.

### [Cu(6)$_2$][PF$_6$]

[Cu(**6**)$_2$][PF$_6$] was isolated as red crystals (25 mg, 91%). $^1$H NMR (500 MHz, $CD_2Cl_2$) $\delta$ (ppm) 8.49 (ddd, $J$ = 5.0, 1.5, 0.8 Hz, 2H, $H^{A6}$), 8.34 (d, $J$ = 8.2 Hz, 2H, $H^{A3}$), 8.19 (d, $J$ = 8.0 Hz, 2H, $H^{B3}$), 8.10 (td, $J$ = 7.8, 1.6 Hz, 2H, $H^{A4}$), 8.01 (t, $J$ = 7.8 Hz, 2H, $H^{B4}$), 7.55 (ddd, $J$ = 7.5, 5.1, 1.1 Hz, 2H, $H^{A5}$), 7.48 (d, $J$ = 7.7 Hz, 2H, $H^{B5}$), 2.26 (s, 6H, $H^{Me}$); $^{13}$C{$^1$H} NMR (126 MHz, $CD_2Cl_2$) $\delta$ (ppm) 158.1 ($C^{B6}$), 152.9 ($C^{A2}$), 151.9 ($C^{B2}$), 149.3 ($C^{A6}$), 138.8 ($C^{B4}$), 138.6 ($C^{A4}$), 126.8 ($C^{A5}$), 126.6 ($C^{B5}$), 122.6 ($C^{A3}$), 119.6 ($C^{B3}$), 25.6 ($C^{Me}$); IR (solid, $\nu$/cm$^{-1}$) 3080 w, 2920 w, 2853 w, 2361 w, 2336 w, 1653 w, 1595 w, 1558 w, 1558 w, 1452 s, 1379 w, 1300 w, 1252 w, 1238 w, 1180 w, 1161 w, 1101 w, 1053 w, 1009 w, 910 w, 876 w, 827 s, 812 s, 766 s, 723 w, 652 w, 631 w. UV/VIS ($CH_2Cl_2$, $1.0 \times 10^{-4}$ mol dm$^{-3}$) $\lambda_{max}$/nm 249 ($\varepsilon$/dm$^3$ mol$^{-1}$ cm$^{-1}$ 20 000), 265 (25 600), 295 (32 200), sh 309 (20 000), 458 (6400), 530 (1400). ESI MS: *m/z* 403.2 $[M - PF_6]^+$ (base peak, calc. 403.1). Found C 48.27, H 3.81, N 10.05; $C_{22}H_{20}CuF_6N_4P$ requires C 48.14, H 3.67, N 10.21%.

### Crystal structure determinations

Data were collected on a Bruker-Nonius KappaAPEX diffractometer, with data reduction, solution and refinement using the programs APEX2,[40] SIR92[41] and CRYSTALS,[42] or on a Stoe IPDS diffractometer with data reduction, solution and refinement using Stoe IPDS software[43] and SHELXL97.[44] ORTEP figures were drawn using Ortep-3 for Windows,[45] and structures were analysed with the program Mercury v. 2.3.[46,47]

### Ligand 3

$C_{15}H_{13}N_3$, $M$ = 235.29, colourless block, triclinic, space group $P\bar{1}$, $a$ = 8.9873(7), $b$ = 10.3479(7), $c$ = 12.9086(10) Å, $\alpha$ = 98.400(4), $\beta$ = 99.933(4), $\gamma$ = 90.639(4)°, $U$ = 1169.00(15) Å$^3$, $Z$ = 4, $D_c$ = 1.337 Mg m$^{-3}$, $\mu$(Mo-K$\alpha$) = 0.082 mm$^{-1}$, $T$ = 123 K. Total 32 162 reflections, 7705 unique, $R_{int}$ = 0.033. Refinement of 6116 reflections (325 parameters) with $I > 2\sigma(I)$ converged at final $R_1$ = 0.0832 ($R1$ all data = 0.0923), w$R_2$ = 0.0787 ($wR2$ all data = 0.1079), gof = 0.9314.

### Ligand 4

$C_{14}H_{10}N_2Se$, $M$ = 285.21, colourless needle, orthorhombic, space group $Pna2_1$, $a$ = 10.715(5), $b$ = 19.191(8), $c$ = 5.731(3) Å, $U$ = 1178.4(9) Å$^3$, $Z$ = 4, $D_c$ = 1.608 Mg m$^{-3}$, $\mu$(Mo-K$\alpha$) = 3.162 mm$^{-1}$, $T$ = 123 K. Total 19 837 reflections, 2811 unique, $R_{int}$ = 0.092. Refinement of 1755 reflections (155 parameters) with $I > 2\sigma(I)$ converged at final $R_1$ = 0.0458 ($R1$ all data = 0.0774), w$R_2$ = 0.0421 ($wR2$ all data = 0.0805), gof = 1.102.

### [Cu(1)$_2$][PF$_6$]

$C_{28}H_{20}CuF_6N_4O_2P$, $M$ = 653.00, red plate, monoclinic, space group $P2_1/c$, $a$ = 11.6298(5), $b$ = 8.6881(3), $c$ = 13.7113(6) Å, $\beta$ = 107.915(2)°, $U$ = 1318.23(9) Å$^3$, $Z$ = 2, $D_c$ = 1.645 Mg m$^{-3}$, $\mu$(Mo-K$\alpha$) = 0.967 mm$^{-1}$, $T$ = 123 K. Total 61 626 reflections, 9825 unique, $R_{int}$ = 0.036. Refinement of 8405 reflections (191 parameters) with $I > 2\sigma(I)$ converged at final $R_1$ = 0.0394 ($R1$ all data = 0.0470), w$R_2$ = 0.0354 ($wR2$ all data = 0.0613), gof = 0.9996.

### [Cu(2)$_2$][PF$_6$]

$C_{28}H_{20}CuF_6N_4PS_2$, $M$ = 685.13, red block, triclinic, space group $P\bar{1}$, $a$ = 7.1898(2), $b$ = 14.0902(3), $c$ = 14.6598(4) Å, $\alpha$ = 103.270(2), $\beta$ = 99.206(2), $\gamma$ = 98.373(2)°, $U$ = 1400.92(7) Å$^3$, $Z$ = 2, $D_c$ = 1.624 Mg m$^{-3}$, $\mu$(Mo-K$\alpha$) = 1.053 mm$^{-1}$, $T$ = 123 K. Total 22 905 reflections, 7740 unique, $R_{int}$ = 0.046. Refinement of 4821 reflections (114 parameters) with $I > 2\sigma(I)$ converged at final $R_1$ = 0.0404 ($R1$ all data = 0.0770), w$R_2$ = 0.0389 ($wR2$ all data = 0.0696), gof = 1.0610.

### [Cu(3)$_2$][PF$_6$]

$C_{30}H_{26}CuF_6N_6P$, $M$ = 679.08, red block, monoclinic, space group $C2/c$, $a$ = 15.5702(6), $b$ = 12.5528(5), $c$ = 15.1905(6) Å, $\beta$ = 102.575(2)°, $U$ = 2897.8(2) Å$^3$, $Z$ = 4, $D_c$ = 1.556 Mg m$^{-3}$, $\mu$(Mo-K$\alpha$) = 0.880 mm$^{-1}$, $T$ = 123 K. Total 79 592 reflections, 7731 unique, $R_{int}$ = 0.040. Refinement of 6961 reflections (200 parameters) with $I > 2\sigma(I)$ converged at final $R_1$ = 0.0319 ($R1$ all data = 0.0345), w$R_2$ = 0.0339 ($wR2$ all data = 0.0466), gof = 1.0580.

### [Cu(5)$_2$][PF$_6$]

$C_{32}H_{24}CuF_6N_4P$, $M$ = 673.07, red plate, monoclinic, space group $C2/c$, $a$ = 8.0516(13), $b$ = 27.170(6), $c$ = 13.159(2) Å, $\beta$ = 96.239(13)°, $U$ = 2861.7(9) Å$^3$, $Z$ = 4, $D_c$ = 1.562 Mg m$^{-3}$, $\mu$(Mo-K$\alpha$) = 0.889 mm$^{-1}$, $T$ = 173 K. Total 22 088 reflections, 3452 unique, $R_{int}$ = 0.0572. Refinement of 3218 reflections (201 parameters) with $I > 2\sigma(I)$ converged at final $R_1$ = 0.0358 ($R1$ all data = 0.0390), w$R_2$ = 0.0944 ($wR2$ all data = 0.0967), gof = 1.073.

### [Cu(6)$_2$][PF$_6$]

$C_{22}H_{20}CuF_6N_4P$, $M$ = 548.94, red block, triclinic, space group $P\bar{1}$, $a$ = 7.7042(8), $b$ = 10.2596(11), $c$ = 15.3283(14) Å, $\alpha$ = 107.978(8), $\beta$ = 97.393(8), $\gamma$ = 100.067(8)°, $U$ = 1112.90(19) Å$^3$, $Z$ = 2, $D_c$ = 1.638 Mg m$^{-3}$, $\mu$(Mo-K$\alpha$) = 1.122 mm$^{-1}$, $T$ = 173 K. Total 23 465 reflections, 4574 unique, $R_{int}$ = 0.0547. Refinement of 4378 reflections (309 parameters) with $I > 2\sigma(I)$ converged at final

$R_1 = 0.0414$ ($R1$ all data = 0.0428), w$R_2 = 0.1117$ ($wR2$ all data = 0.1130), gof = 1.049.

### Preparation of solar cells

Nanocrystalline $TiO_2$ electrodes were prepared by doctor blading a colloidal $TiO_2$ paste (Solaronix Nanooxide-T, colloidal anatase) onto a conducting glass slide (F-doped $SnO_2$, FTO, Hartford glass company, Tec 8, 8 Ω $cm^{-2}$) to produce a film 6 μm thick. After annealing at 450 °C for 30 min, each slide was cooled to ≈80 °C and dipped into a DMSO solution of ligand **7**, **8**, **9** or **10** (3 mmol $dm^{-3}$) overnight. The colourless slide was then removed from the solution, washed with DMSO and then EtOH, and dried. The functionalized electrode was then dipped into an EtOH solution of $[CuL_2]^+$ (L = **1–6**) (1 mmol $dm^{-3}$) and left to stand for 24 h during which time the slide became red in colour. The slide was removed from the solution, and was washed with EtOH. The solar cells were made using LiI (0.5 mol $dm^{-3}$), $I_2$ (0.05 mol $dm^{-3}$), 1-methylbenzimidazole (0.5 mol $dm^{-3}$) and 1-butyl-3-methylimidazolinium iodide (0.6 mol $dm^{-3}$) in 3-methoxypropionitrile as electrolyte, the latter being chosen to produce the best comparison with the state-of-the-art optimized systems based on N719 (standard dye purchased from Solaronix). Cathodes (size-matched to the anodes) were constructed from FTO glass pieces platinized using $H_2PtCl_6$ (5 mmol $dm^{-3}$) in propan-2-ol, followed by heating to 280 °C for 15 min. The anode and cathode were assembled using Surlyn (Dupont) plastic by heating while pressing them together. Measurements were made by irradiating from behind using a light source SolarSim 150 (100 mW $cm^{-2}$ = 1 sun).

## Results and discussion

### Ligand synthesis and characterization

Three of the general strategies for the preparation of 6-aryl-2,2′-bipyridines are Kröhnke methodology,[31] direct coupling of a lithiated aryl compound and bpy,[34] and Jameson's strategy.[36,48] The choice between these routes depends upon the substituent. Furyl derivative **1** is most efficiently synthesized by the Kröhnke route as detailed by Lee and coworkers.[32] Ligand **2** has previously been prepared using a Kröhnke synthesis,[23,35] but we have found it more convenient to use a one-pot method using direct coupling of 2-lithiothiophene (prepared *in situ*)[49] and 2,2′-bipyridine, following the general strategy used by Sauvage and coworkers for the preparation of 2,2′-bipyridines and 2,9-disubstituted 1,10-phenanthrolines.[34] In contrast to **1** and **2**, pyrrolyl derivative **3** and selenopheneyl derivative **4** have not previously been reported.

6-(3,5-Diphenyl-2-pyrrolyl)-2,2′-bipyridine has been prepared in 67% yield by Nagata *et al.* using a Kröhnke synthesis.[50] Overall yields of 10–40% were obtained for **3** using a multi-step Kröhnke synthesis over a period of 4–7 days. Using a two-step Jameson strategy, yields of **3** of up to 50% were achieved, but again, reaction and purification required a week. We therefore turned to the one-pot reaction of 1-methylpyrrole and $^n$BuLi at 223 K, followed by treatment with bpy at 273–295 K which led, after workup and purification, to **3** which was isolated as a white crystalline solid. The yield of 15.4% was disappointing, but the method was significantly more efficient in terms of time (<3 days) than either of the Kröhnke or Jameson routes. The base peak in the EI mass spectrum of **3** appeared at $m/z$ 234.1 and was assigned to $[M - H]^+$. The intensity of the peak at $m/z$ 235.1 was too great to arise only from $^{13}C$ in the $[M - H]^+$ ion and so was assigned to a combination of the latter and the parent ion $[M]^+$. The $^1H$ and $^{13}C$ NMR spectra were assigned by 2D methods. In the NOESY spectrum, cross peaks between the signals for $H^{C3}$ and $H^{B5}$, and for $H^{C5}$ and $H^{Me}$ (see Scheme 1) permitted resonances for $H^{C3}$ and $H^{C5}$ to be unambiguously assigned.

Single crystals of **3** were grown by slow evaporation of a hexane solution of the ligand. X-Ray diffraction confirmed the structure depicted in Fig. 1. The compound crystallizes in the triclinic $P\bar{1}$ space group with the asymmetric unit containing two independent, but structurally similar, molecules (A and B). The bpy domain adopts the expected *trans*-configuration with the two rings in each unit deviating slightly from planarity (angles between the least squares planes in independent molecules A and B are 14.14(8) and 5.79(8)°, respectively). The pyrrole ring lies close to the bpy plane (angles between the least squares planes of rings containing atoms N2 and N3, and corresponding rings in molecule B, are 3.19(9) and 11.62(9)°). The orientation of the pyrrole ring is such that the methyl substituent faces the lone pair of atom N2 (Fig. 1), and similarly in the second independent molecule. The methyl H atoms are too distant from N2 for there to be weak C–H···N interactions. Thus, the preference for the observed orientation is presumably associated with minimizing repulsive H···H interactions while maintaining an approximately planar molecular geometry to optimize intermolecular interactions. The crystal packing is such that pairs of molecules A associate through face-to-face π-stacking across an inversion centre, and similarly for pairs of molecules B. The centroid···plane distances are 3.37 and 3.30 Å, for A and B, respectively. Molecules further assemble into ribbons through weak $CH_{pyrrole}\cdots N_{bpy}$ hydrogen bonds (C14H141···N1$^i$ = 2.62, C14···N1$^i$ = 3.579(2) Å, C14–H141···N1$^i$ = 176°, symmetry code i = $x$, 1 + $y$, $z$ between molecules A; corresponding parameters for molecules B are C29H291···N4$^{ii}$ = 2.69, C29···N4$^{ii}$ = 3.655(2) Å, C29–H291···N4$^{ii}$ = 175°, symmetry code ii = $x$, −1 + $y$, $z$). The two sets of ribbons are approximately orthogonal to one another (Fig. 2).

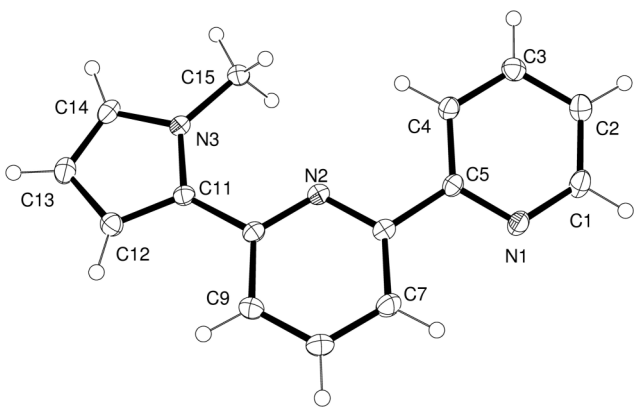


**Fig. 1** Structure of one (molecule A) of two independent molecules of **3**; ellipsoids plotted at 40% probability level. Selected bond lengths and angles: N1–C1 = 1.338(2), N1–C5 = 1.347(2), N2–C6 = 1.3460(19), N2–C10 = 1.341(2), N3–C11 = 1.3866(19), N3–C14 = 1.372(2), N3–C15 = 1.460(2) Å; C11–N3–C14 = 109.00(13), C11–N3–C15 = 128.76(13), C14–N3–C15 = 122.20(14)°.

 

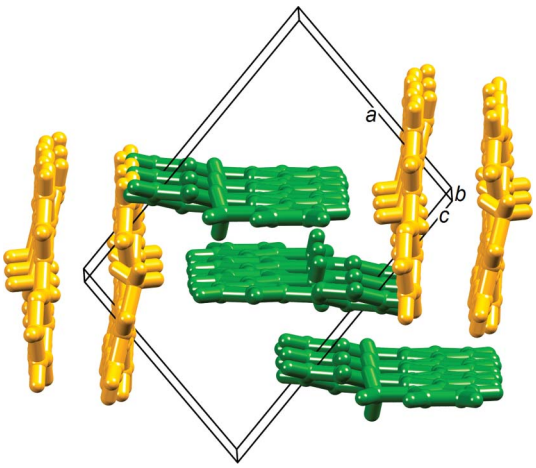


**Fig. 2** Part of the packing diagram for **3**. Ribbons of molecules A and B are shown in green and orange, respectively.

Since the lithiation route was successful for the preparation of **3**, we also chose this strategy to synthesize compound **4**. Treatment of selenophene with $^{n}$BuLi followed by bpy resulted in the isolation of **4** in 28% after workup. The electrospray mass spectrum exhibited peaks at $m/z$ 309.0 and 287.3 corresponding to $[M + Na]^+$ and $[M + H]^+$, and the isotope distributions were consistent with those calculated. The $^1$H and $^{13}$C NMR spectra were in accord with the structure shown in Scheme 1 and were fully assigned by 2D methods. The $^1$H NMR resonance for $H^{C5}$ (*i.e.* the proton closest to the Se atom) exhibited satellites with coupling to $^{77}$Se of 45 Hz. In the $^{77}$Se{$^1$H} NMR spectrum, a single resonance at $\delta$ 603.1 ppm was observed.

Crystals of **4** suitable for X-ray diffraction grew overnight by evaporation of an $Et_2O$ solution of the compound, and Fig. 3 depicts the structure. The molecule is planar (angles between the least squares planes of the rings containing N1/N2 and N2/Se1 are 3.4(3) and 5.2(3)°) and fully ordered. The bpy domain is in the expected *trans*-configuration. The orientation of the selenium-containing heterocycle results in an Se1 ··· N2 separation of 2.982(5) Å (compare the sum of the van der Waals radii of 3.54 Å). The observed separation is shorter than intramolecular Se ··· N contacts observed in related molecules: 3.490(2) Å in 2-((mesitylselanyl)methyl)quinoline,[51] 3.406(2) Å in 1,3-bis(2-pyridylmethyl)triselane,[51] and 3.448(4) Å in 2,6-bis((phenylselanyl)methyl)pyridine.[52] Significantly, **4** adopts an analogous conformation to **2** in which the S ··· N separation in the solid state is 2.895(3) Å.[30] Both **4** and its sulfur analogue[30] crystallize in the space group $Pna2_1$ with similar cell dimensions, and the molecular packing in the two compounds is essentially the same involving C–H ··· π and C–H ··· N interactions. Despite the planarity of ligands **2** and **4**, there is no face-to-face π-stacking.

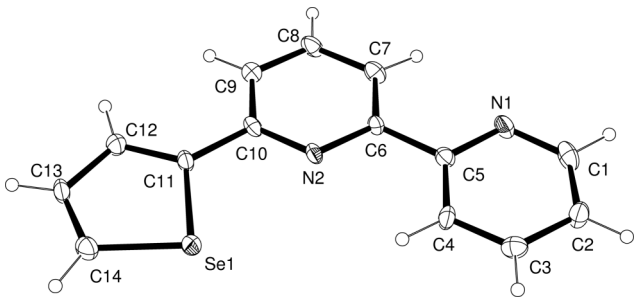


**Fig. 3** Structure of **4**; ellipsoids plotted at 30% probability level. Selected bond lengths and angles: C11–Se1 = 1.864(7), C14–Se1 = 1.866(7), C1–N1 = 1.333(9), C5–N1 = 1.340(8), C6–N2 = 1.359(6), C10–N2 = 1.328(8) Å; C5–N1–C1 = 116.8(6), C6–N2–C10 = 118.3(5), C14–Se1–C11 = 86.3(3)°.

**Table 1** Selected bond parameters for the homoleptic copper(I) complexes. In each of $[Cu(\mathbf{1})_2]^+$ and $[Cu(\mathbf{3})_2]^+$, the two ligands are related by a 2-fold axis

| | $[Cu(\mathbf{1})_2][PF_6]$ | $[Cu(\mathbf{2})_2][PF_6]^a$ | $[Cu(\mathbf{3})_2][PF_6]$ |
|---|---|---|---|
| | atom X = O1 | atom X = S1, S2 | Atom X = N3 |
| Bond distance/Å | | | |
| Cu1–N1 | 2.0046(6) | 1.980(2) | 1.9918(6) |
| Cu1–N2 | 2.0932(5) | 2.200(2) | 2.0758(6) |
| Cu1–N3/N1$^i$ | 2.0046(6) | 2.006(2) | 1.9918(6) |
| Cu1–N4/N2$^i$ | 2.0932(5) | 2.095(2) | 2.0758(6) |
| C11–X | 1.3759(8) | 1.720(3) | 1.3800(10) |
| C14–X | 1.3690(10) | 1.712(3) | 1.3713(11) |
| C31–X | | 1.7111(6) | |
| C34–X | | 1.7001(4) | |
| Bond angle/deg | | | |
| N1–Cu1–N2 | 81.05(2) | 80.41(8) | 81.43(2) |
| N1–Cu1–N3/N1$^i$ | 124.53(4) | 128.44(9) | 134.50(4) |
| N2–Cu1–N3/N1$^i$ | 137.70(2) | 133.10(8) | 129.55(2) |
| N1–Cu1–N4/N2$^i$ | 137.70(2) | 143.07(9) | 129.55(2) |
| N2–Cu1–N4/N2$^i$ | 102.26(3) | 94.74(8) | 101.79(3) |
| N3/N1$^i$ –Cu1–N4/N2$^i$ | 81.05(2) | 80.97(9) | 81.43(2) |
| C11–X–C14 | 106.59(6) | 92.14(16) | 108.77(7) |
| C31–X–C34 | | 92.690(9) | |

[a] Major occupancy atoms only included.

### Homoleptic copper(I) complexes with heteroaromatic substituents

The reactions of ligands **1**, **2**, **3** or **4** with $[Cu(NCMe)_4][PF_6]$ in MeCN at room temperature were monitored by thin layer chromatography and each was complete within two hours. Complexes $[Cu(\mathbf{1})_2][PF_6]$, $[Cu(\mathbf{2})_2][PF_6]$ and $[Cu(\mathbf{4})_2][PF_6]$ were isolated in near quantitative yields, and $[Cu(\mathbf{3})_2][PF_6]$ in 74% yield. The electrospray mass spectrum of each complex exhibited a peak envelope corresponding to $[M - PF_6]^+$ with an isotope distribution matching that simulated. Single crystals of $[Cu(\mathbf{1})_2][PF_6]$, $[Cu(\mathbf{2})_2][PF_6]$, $[Cu(\mathbf{3})_2][PF_6]$ were grown by recrystallization from EtOH, by layering a $CHCl_3$ solution of the compound with toluene, and from a $CH_2Cl_2/Et_2O$ solution kept at 2 °C, respectively. All three complexes crystallize without solvent, and the structures and packing can therefore be directly compared. Fig. 4–6 illustrate the structures of the $[Cu(\mathbf{1})_2]^+$, $[Cu(\mathbf{2})_2]^+$ and $[Cu(\mathbf{3})_2]^+$ cations, and important bond lengths and angles are given in Table 1. $[Cu(\mathbf{1})_2][PF_6]$ and $[Cu(\mathbf{3})_2][PF_6]$ crystallize in monoclinic space groups $P2_1/c$ and $C2/c$, respectively, and the two ligands in each of $[Cu(\mathbf{1})_2]^+$ and $[Cu(\mathbf{3})_2]^+$ are related by a 2-fold axis passing through atom Cu1. In $[Cu(\mathbf{2})_2][PF_6]$, one of the two ligands suffers from a 2-fold rotational disorder of the thienyl substituent. This has been modelled over two positions with fractional occupancies of 0.869(2) and 0.131(2). Only the major occupancy site is considered in Fig. 5 and Table 1. The hexafluoridophosphate anion in each structure is ordered.

Inspection of the bond distances in Table 1 shows that the Cu1–N2 bond in $[Cu(\mathbf{2})_2][PF_6]$ is noticeably longer (2.200(2) Å) than

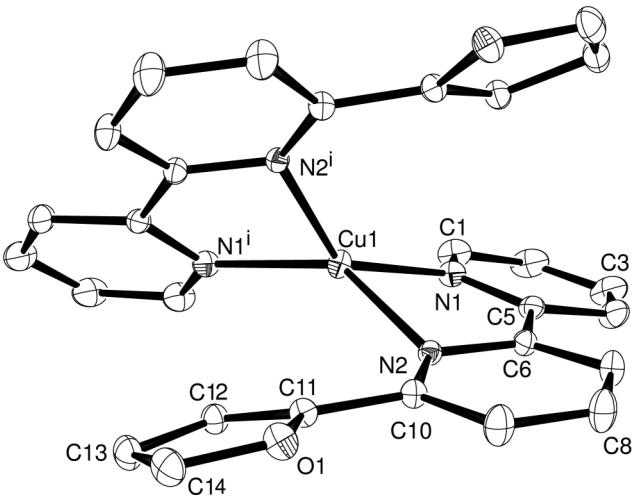


**Fig. 4** Structure of the $[Cu(\mathbf{1})_2]^+$ cation in $[Cu(\mathbf{1})_2][PF_6]$ with H atoms omitted (ellipsoids plotted at 40% probability level). Symmetry code i = 1 − *x*, *y*, $^3/_2$ − *z*.

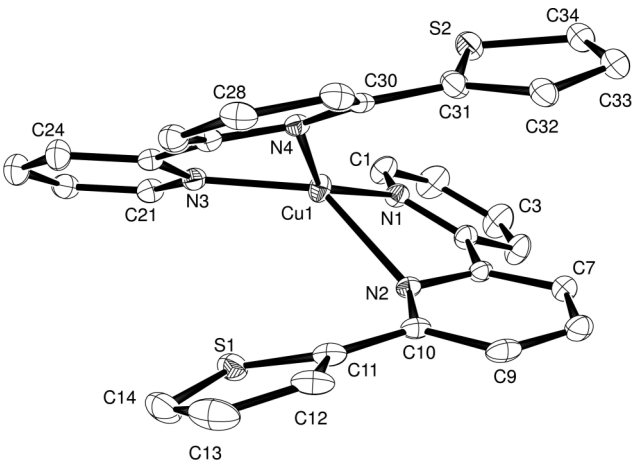


**Fig. 5** Structure of the $[Cu(\mathbf{2})_2]^+$ cation in $[Cu(\mathbf{1})_2][PF_6]$ with H atoms omitted (ellipsoids plotted at 40% probability level). The ring containing atom S2 is disordered and only the major occupancy site is illustrated.

the remaining Cu–N bonds, all of which are close to 2.0 Å. The elongation is associated with a deformation of the corresponding bpy ligand away from planarity: the angle between the least squares planes of the two rings in this copper-bound bpy is 27.16(14)° compared to 16.36(13)° for the second bpy in $[Cu(\mathbf{2})_2]^+$, 14.62(4)° in $[Cu(\mathbf{1})_2]^+$ and 8.54(4)° in $[Cu(\mathbf{3})_2]^+$. As a result of these structural changes, each thienyl substituent in the $[Cu(\mathbf{2})_2]^+$ cation engages in face-to-face π-stacking with the central pyridine ring of the second ligand, the thienyl centroid · · · pyridine plane separations being 3.55 and 3.58 Å.

Preliminary crystallographic data were obtained for $[Cu(\mathbf{4})_2][PF_6]$, but problems with twinning resulted in a poorly refined dataset. We are, however, able to confirm the gross structural features of the cation. The copper(I) ion is in a flattened tetrahedral environment with Cu–N bond distances in the range ≈1.9 to 2.0 Å. Both selenophene-2-yl substituents are rotationally disordered over two positions, but in each ring, one position is dominant. Considering only the major occupancy

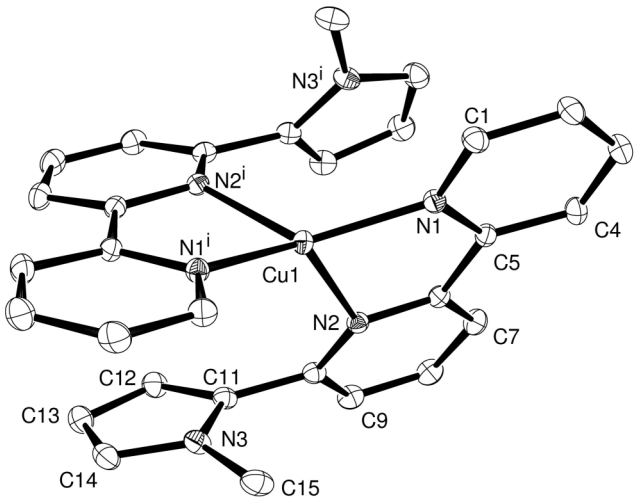


**Fig. 6** Structure of the $[Cu(\mathbf{3})_2]^+$ cation in $[Cu(\mathbf{3})_2][PF_6]$ with H atoms omitted (ellipsoids plotted at 40% probability level). Symmetry code i = 1 − *x*, *y*, $^3/_2$ − *z*.

sites, the orientation of one of the heterocyclic rings permits a short Cu · · · Se contact of ≈3.2 Å.

The extent of inter-ligand π-stacking within each cation is illustrated in Fig. 7. In $[Cu(\mathbf{1})_2][PF_6]$, each furyl group is twisted 16.36(4)° with respect to the plane of the pyridine ring to which it is attached, but as Fig. 7a shows, the mutual twisting of the heterocyclic rings within the ligands does not result in inter-ligand stacking within the $[Cu(\mathbf{1})_2]^+$ cation. We have already noted that in $[Cu(\mathbf{2})_2]^+$, both thienyl substituents are involved in intra-cation face-to-face interactions (Fig. 7b). However, the most effective intramolecular aryl embrace is achieved in $[Cu(\mathbf{3})_2]^+$, despite the presence of the *N*-methyl substituents. Each pyrrolyl unit twists 54.87(4)° out of the plane of the central pyridine ring in coordinated **3**. The ligand attains a conformation that permits a face-to-face π-interaction between the pyrrolyl domain of one ligand and the central pyridine ring of the other: the interplane angle is 2.8° and the pyrrolyl centroid · · · pyridine plane separation is 3.46 Å.

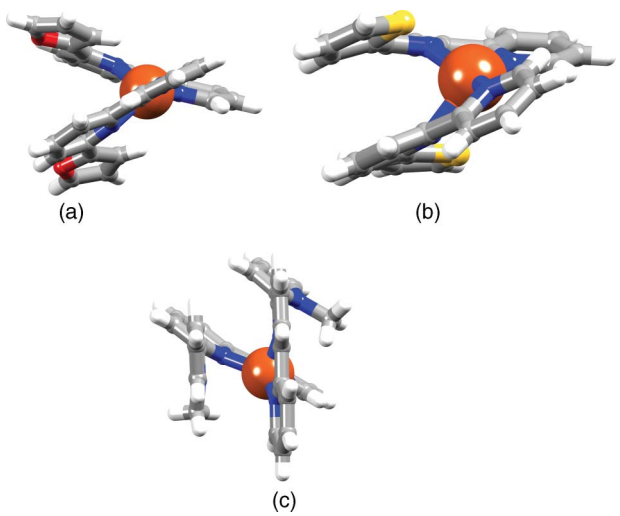


**Fig. 7** Representations of the (a) $[Cu(\mathbf{1})_2]^+$, (b) $[Cu(\mathbf{2})_2]^+$, and (c) $[Cu(\mathbf{3})_2]^+$ cations, illustrating the enhancement of inter-ligand face-to-face π-interactions on going from furyl to thienyl to pyrrolyl substituent.

 

The crystal packing in all three complexes involves extensive cation···anion CH···F contacts and some degree of inter-cation π-stacking, although in $[Cu(\mathbf{2})_2][PF_6]$ this is rather inefficient.

At room temperature, signals in the the $CD_2Cl_2$ solution $^1H$ NMR spectra of $[Cu(\mathbf{1})_2][PF_6]$, $[Cu(\mathbf{2})_2][PF_6]$, $[Cu(\mathbf{3})_2][PF_6]$ and $[Cu(\mathbf{4})_2][PF_6]$ are broadened (Fig. 8a–8d), in particular those of the thienyl derivative (Fig. 8b). The spectra are better resolved at low temperatures. These observations may arise from slow rotation of the heteroaromatic substituent about the $C_{bpy}$–$C_{hetero}$ bond. However, if this is the case, it initially appears surprising that the most bulky substituent, *i.e.* the *N*-methylpyrrole in $[Cu(\mathbf{3})_2][PF_6]$, presents the least broadened spectrum, and that a sharp, well-resolved spectrum is observed for $[Cu(\mathbf{5})_2][PF_6]$ (Fig. 8e, discussed below). An alternative explanation is that the heteroatom in ligands **1**, **2** and **4** interacts with the copper(I) centre as observed in the solid state for $[Cu(\mathbf{4})_2][PF_6]$, and that this interaction hinders the rotation of the O-, S- and Se-containing substituents. A detailed study of the dynamics of these and model systems is in progress.

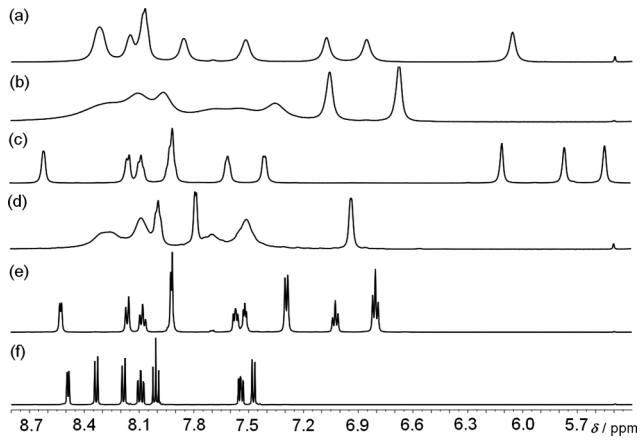


**Fig. 8** Room temperature 500 MHz NMR spectra ($\delta$ 8.8–5.4 ppm) of $CD_2Cl_2$ solutions of (a) $[Cu(\mathbf{1})_2][PF_6]$, (b) $[Cu(\mathbf{2})_2][PF_6]$, (c) $[Cu(\mathbf{3})_2][PF_6]$, (d) $[Cu(\mathbf{4})_2][PF_6]$, (e) $[Cu(\mathbf{5})_2][PF_6]$ and (f) $[Cu(\mathbf{6})_2][PF_6]$. The signal at $\delta$ 5.49 ppm in some of the spectra is one of the $^{13}C$ satellites from $CDHCl_2$.

### Homoleptic copper(I) complexes containing 6-Phbpy or 6-Mebpy

Treatment of $[Cu(NCMe)_4][PF_6]$ with two equivalents of ligand **5** or **6** (Scheme 1) resulted in the isolation of red crystalline $[Cu(\mathbf{5})_2][PF_6]$ or $[Cu(\mathbf{6})_2][PF_6]$ in ≈90% yield. The base peak in the ESI mass spectra of the complexes arose from the $[M - PF_6]^+$ ion (*m*/*z* 527.2 and 403.2, respectively) and the isotope patterns matched those simulated.

Single crystals of $[Cu(\mathbf{5})_2][PF_6]$ and $[Cu(\mathbf{6})_2][PF_6]$ were grown from $CH_2Cl_2$ solutions of the complexes layered with $Et_2O$. The structures of the $[Cu(\mathbf{5})_2]^+$ and $[Cu(\mathbf{6})_2]^+$ cations are depicted in Fig. 9 and 10, and bond parameters for the metal coordination spheres are listed in the figure captions. The copper(I) coordination sphere in $[Cu(\mathbf{6})_2]^+$ is close to tetrahedral, with the angle between the two bpy domains being 87.31(3)° (Fig. 11a). In contrast, Fig. 11b illustrates significant flattening of the ligand arrangement, the corresponding angle being 65.47(2)°. The difference originates in intra-cation arene stacking in $[Cu(\mathbf{5})_2]^+$. The phenyl substituent of one ligand **5** (twisted 45.02(10)° with respect to the bpy unit) lies over the pyridine ring containing N2 of the second ligand.

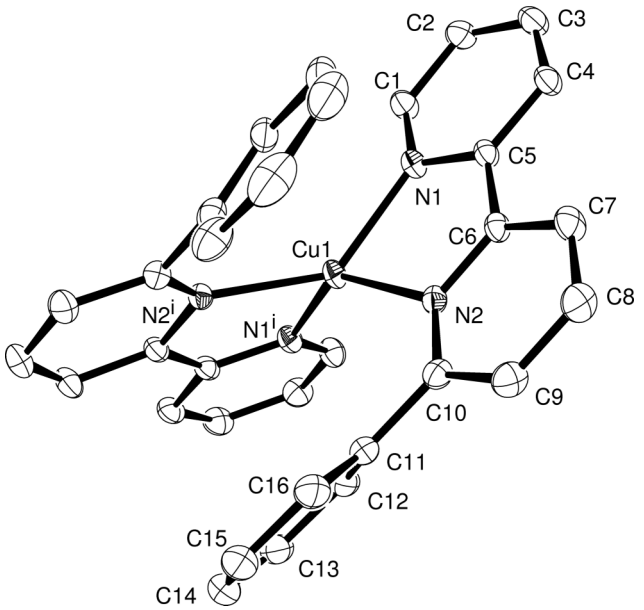


**Fig. 9** Structure of the $[Cu(\mathbf{5})_2]^+$ cation in $[Cu(\mathbf{5})_2][PF_6]$ with H atoms omitted (ellipsoids plotted at 30% probability level). Symmetry code i = 1 − *x*, *y*, $^3/_2$ − *z*. Selected bond parameters: Cu1–N1 = 2.0278(14), Cu1–N2 = 2.0530(14) Å; N1–Cu1–N2 = 80.82(6), N1-Cu1–$N1^i$ = 119.11(8), N1–Cu1–$N2^i$ = 135.29(6), $N1^i$–Cu1–$N2^i$ = 80.82(6), N2–Cu1–$N2^i$ = 114.09(8)°.

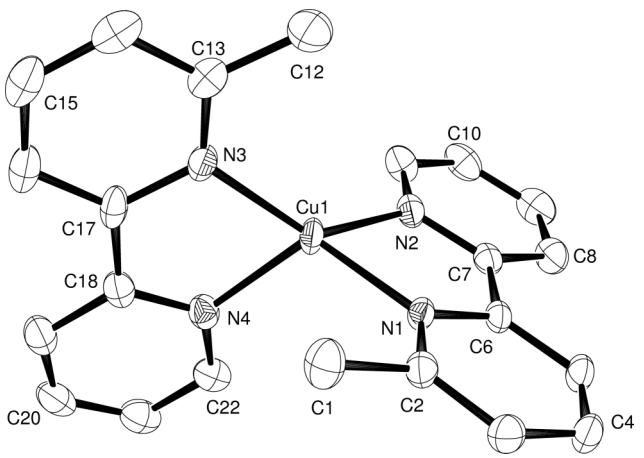


**Fig. 10** Structure of the $[Cu(\mathbf{6})_2]^+$ cation in $[Cu(\mathbf{6})_2][PF_6]$ with H atoms omitted (ellipsoids plotted at 30% probability level). Selected bond parameters: Cu1–N3 = 1.996(2), Cu1–N2 = 1.998(2), Cu1–N4 = 2.044(2), Cu1–N1 = 2.0443(18) Å; N3–Cu1–N2 = 137.88(9), N3–Cu1–N4 = 81.64(9), N2–Cu1–N4 = 116.07(9), N3–Cu1–N1 = 126.69(8), N2–Cu1–N1 = 81.78(8), N4–Cu1–N1 = 115.82(8)°.

Although there is a face-to-face π-interaction (centroid to ring distance = 3.66 Å), it is not optimal since the planes of the two rings subtend an angle of 10.8° with one another. The crystal packing in $[Cu(\mathbf{5})_2][PF_6]$ is dominated by C–H···F contacts rather than π-stacking interactions. In contrast, the packing in $[Cu(\mathbf{6})_2][PF_6]$ involves efficient face-to-face π-stacking between centrosymmetric pairs of cations, involving bpy domains containing atoms N3/N4 and N3i/N4i (symmetry code i = 1 − *x*, 1 − *y*, 1 − *z*; inter-plane separation = 3.36 Å). Extension of the π-stacking between bpy units of adjacent cations involving N3/N4 and N3ii/N4ii

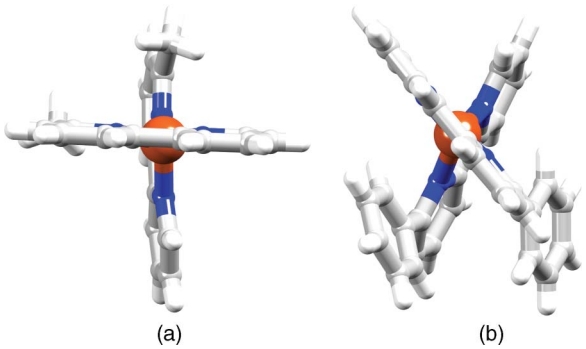


**Fig. 11** Comparison of the coordination spheres in (a) $[Cu(\mathbf{6})_2]^+$ and (b) $[Cu(\mathbf{5})_2]^+$ in the hexafluoridophosphate salts.

(symmetry code ii = 2 – $x$, 2 – $y$, 2 – $z$; inter-plane distance = 3.29 Å) results in the propagation of chains slicing obliquely through the unit cell.

### Electronic absorption spectroscopy

The electronic absorption spectra of $CH_2Cl_2$ solutions of $[CuL_2][PF_6]$ with L = **1–6** (Fig. 12) exhibit high energy absorption bands arising from ligand-based $\pi^* \leftarrow \pi$ transitions. For each complex, two broad absorptions with values of $\varepsilon_{max}$ ranging from 1700 to 3800 $dm^3\ mol^{-1}\ cm^{-1}$ are observed around 400–435 nm and 513–550 nm and are assigned to MLCT transitions.

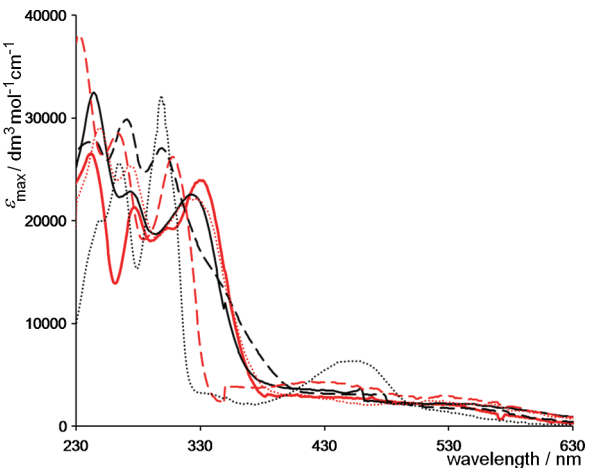


**Fig. 12** Electronic absorption spectra of $CH_2Cl_2$ solutions of $[CuL_2][PF_6]$ for L = **1–6**. Key: Solid red line, L = **1**; solid black line, L = **2**, hashed black line, L = **3**; dotted red line, L = **4**, hashed red line, L = **5**; dotted black line L = **6**. See experimental section for solution concentrations.

### DSCs with heteroleptic copper(I) complexes

Complexes for use as dyes in DSCs incorporate substituents that anchor the complex to the $TiO_2$ semiconductor surface, and carboxylate and phosphonate functionalities are popular choices. Our recent studies of potential dyes for DSCs have focused on copper(I) complexes incorporating bpy-based and related ligands with carboxylic acid or carboxylate functionalities.[1,4,9] While the synthesis of homoleptic complexes of type $[CuL_2]^+$ is straightforward, the requirement to incorporate anchoring groups limits the range of ligands and, therefore, of complexes that can be screened. The efficient preparation of heteroleptic complexes is therefore of importance. We have demonstrated the lability in solution of diimine and phosphane ligands in copper(I) complexes, and the formation of heteroleptic complexes from equilibrium mixtures of two homoleptic species.[6,17] Following these observations, we have adopted a simple strategy for rapid screening of the performance of heteroleptic copper(I) complexes in DSCs, using a common anchoring ligand, L′, and a variable second ligand, L, which is introduced as $[CuL_2]^+$. In this study, for the assembly of surface-bound $[CuLL']^+$, L′ is one of the ligands **7–10** shown in Scheme 2, and L = **1–6**. Ligands **7–9** contain carboxylic acid (carboxylate) anchoring groups while in **10**, anchoring is through the phosphonic acid (phosphonate) units. Grätzel has established that absorption of dyes onto $TiO_2$ is enhanced by the presence of phosphonate groups.[53]

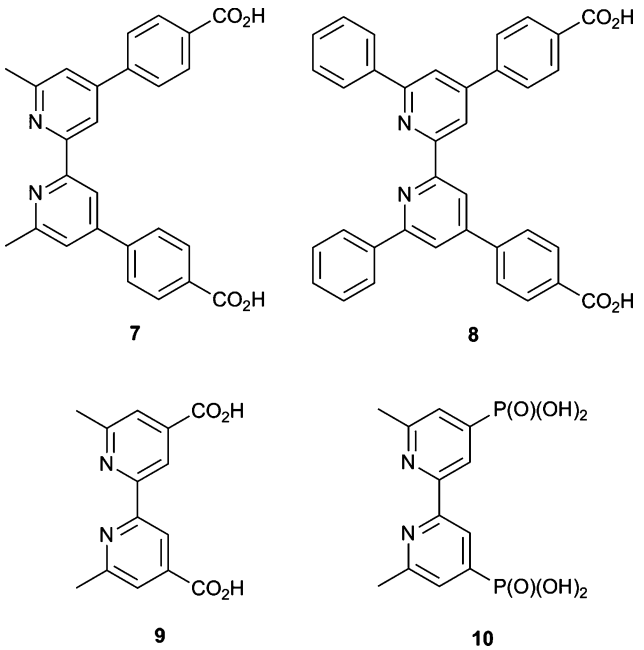


**Scheme 2** Structures of the anchoring ligands, L′, **7–10**. The anchoring groups are the carboxylic or phosphonic acids or their conjugate bases.

The anodes were prepared by dipping annealed conducting glass slides (see experimental section) into a DMSO solution of the anchoring ligand L′ (**7–10**). After washing and drying the slides, the latter were left to stand for 24 h in EtOH solutions of the homoleptic complexes $[CuL_2][PF_6]$ (L = **1–6**), allowing the equilibrium in Scheme 3 to be established. The appearance of the slide changed from colourless to red, consistent with the presence of a surface adsorbed copper(I) complex and the red colour persisted after the slide was washed with EtOH.

The sample prepared with L = **4** and L′ = **10** was subjected to MALDI-TOF mass spectrometric analysis. A sample of red-coloured $TiO_2$ was scratched from the surface of the slide and the powder was suspended in $CH_2Cl_2$ and mixed with the MALDI matrix (2,5-dihydroxybenzoic acid). The mass spectrum showed peaks at $m/z$ 348.8, 634.7 and 762.7 which were assigned to $[Cu(\mathbf{4})]^+$ (calc. 348.9), $[Cu(\mathbf{4})_2]^+$ (calc. 634.9) and $[Cu(\mathbf{4})(\mathbf{10} - 4H + Et + 2Na)]^+$ (calc. 763.9). Isotope patterns consistent with these ions were observed.

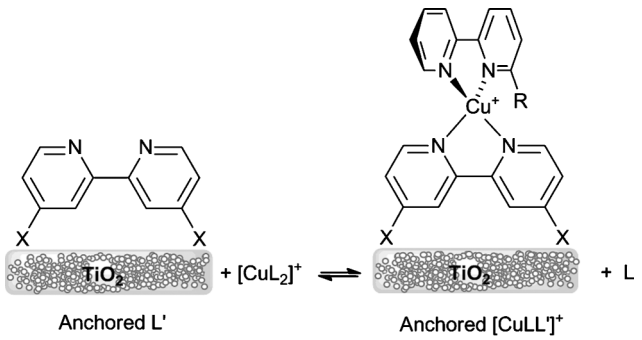


**Scheme 3** Ligand exchange leading to surface anchored heteroleptic copper(I) dyes. L = **1–6**, L′ = **7–10**; X = anchoring group (see Scheme 2).

Diffuse reflectance electronic absorption spectra of the surfaces of the slides were also recorded. Fig. 13 is representative of the results and illustrates the spectra of the $TiO_2$-anchored ligands **7–10** after treatment with $[Cu(\mathbf{3})_2][PF_6]$; corresponding spectra for the remaining 20 devices are given in Fig. S1–S5, ESI.† The spectra were compared to that of a $TiO_2$ electrode which had been dipped into a DMSO solution of the homoleptic complex $[Cu(\mathbf{10})_2]Cl$[54] for four hours. The differences between the spectra shown as solid lines in Fig. 13 provide evidence for the presence of different surface species, and the tail into the visible region is consistent with surface-binding of complexes of copper(I) as opposed to free ligand, the latter being colourless. Although in Fig. 13, the spectra for combinations of **7** and $[Cu(\mathbf{3})_2][PF_6]$, and of **10** and $[Cu(\mathbf{3})_2][PF_6]$ look similar, we can rule out the possibility that the spectra arise from different surface coverages of $[Cu(\mathbf{3})_2][PF_6]$ on the basis that ligand **3** has no anchoring groups. Significantly, each of the spectra for the combinations of **7**, **8**, **9** or **10** after treatment with $[Cu(\mathbf{3})_2][PF_6]$ shows a low energy shoulder which coincides with the dominant band in the diffuse reflectance spectrum of $TiO_2$-supported $[Cu(\mathbf{10})_2]^+$. This further supports the presence of the heteroleptic species.

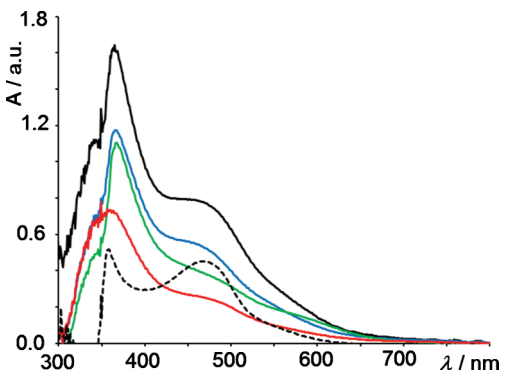


**Fig. 13** Thin layer solid state diffuse reflectance electronic absorption spectra of $TiO_2$-anchored ligands **7** (black), **8** (green), **9** (red) and **10** (blue) after treatment with $[Cu(\mathbf{3})_2][PF_6]$. The hashed line is for $[Cu(\mathbf{10})_2]Cl$.

Table 2 presents the DSC efficiency data for the solar cells and also the data for standard dye N719 measured under the same conditions as the copper(I) complexes. The measurements were made in open cells and the configuration is different to optimized cells reporting >10% efficiency for N719. For a common anchoring ligand L′, changing ligand L leads to only small variations in the efficienices of the solar cells. However, for a common ligand L, the choice of the anchoring ligand has a significant effect on the solar cell efficiency, with ligands **7** and **10** performing the best. Anchoring ligands **9** and **10** differ only in the anchoring groups themselves, *i.e.* $CO_2H$ *versus* $PO(OH)_2$ (or conjugate bases thereof). A comparison of the data confirms that high efficiencies are achieved with the phosphonate binding groups which should be considered the anchors of choice for future DSC design.

**Table 2** DSC efficiency data in comparison to N719 measured under the same conditions (see experimental section). $[CuL_2]^+$ are introduced for surface ligand exchange as hexafluoridophosphate salts

| $[CuL_2]^+$ | L′ | $I_{SC}$/A cm$^{-2}$ | $V_{OC}$/V | ff | η/% |
|---|---|---|---|---|---|
| $[Cu(\mathbf{1})_2]^+$ | **7** | 0.005 | 0.506 | 0.54 | 1.25 |
| $[Cu(\mathbf{1})_2]^+$ | **8** | 0.001 | 0.506 | 0.58 | 0.42 |
| $[Cu(\mathbf{1})_2]^+$ | **9** | 0.001 | 0.451 | 0.62 | 0.40 |
| $[Cu(\mathbf{1})_2]^+$ | **10** | 0.004 | 0.561 | 0.60 | 1.51 |
| $[Cu(\mathbf{2})_2]^+$ | **7** | 0.005 | 0.488 | 0.53 | 1.17 |
| $[Cu(\mathbf{2})_2]^+$ | **8** | 0.001 | 0.414 | 0.62 | 0.22 |
| $[Cu(\mathbf{2})_2]^+$ | **9** | 0.001 | 0.433 | 0.59 | 0.35 |
| $[Cu(\mathbf{2})_2]^+$ | **10** | 0.004 | 0.524 | 0.63 | 1.45 |
| $[Cu(\mathbf{3})_2]^+$ | **7** | 0.005 | 0.524 | 0.45 | 1.21 |
| $[Cu(\mathbf{3})_2]^+$ | **8** | 0.001 | 0.469 | 0.57 | 0.25 |
| $[Cu(\mathbf{3})_2]^+$ | **9** | 0.002 | 0.488 | 0.57 | 0.64 |
| $[Cu(\mathbf{3})_2]^+$ | **10** | 0.004 | 0.579 | 0.57 | 1.34 |
| $[Cu(\mathbf{4})_2]^+$ | **7** | 0.005 | 0.488 | 0.57 | 1.31 |
| $[Cu(\mathbf{4})_2]^+$ | **8** | 0.001 | 0.433 | 0.58 | 0.32 |
| $[Cu(\mathbf{4})_2]^+$ | **9** | 0.002 | 0.433 | 0.65 | 0.49 |
| $[Cu(\mathbf{4})_2]^+$ | **10** | 0.004 | 0.543 | 0.63 | 1.31 |
| $[Cu(\mathbf{5})_2]^+$ | **7** | 0.004 | 0.525 | 0.49 | 1.07 |
| $[Cu(\mathbf{5})_2]^+$ | **8** | 0.001 | 0.506 | 0.56 | 0.39 |
| $[Cu(\mathbf{5})_2]^+$ | **9** | 0.002 | 0.451 | 0.60 | 0.48 |
| $[Cu(\mathbf{5})_2]^+$ | **10** | 0.004 | 0.561 | 0.59 | 1.42 |
| $[Cu(\mathbf{6})_2]^+$ | **7** | 0.005 | 0.506 | 0.55 | 1.28 |
| $[Cu(\mathbf{6})_2]^+$ | **8** | 0.001 | 0.487 | 0.56 | 0.31 |
| $[Cu(\mathbf{6})_2]^+$ | **9** | 0.002 | 0.469 | 0.59 | 0.55 |
| $[Cu(\mathbf{6})_2]^+$ | **10** | 0.004 | 0.561 | 0.56 | 1.20 |
| N719 | | 0.015 | 0.715 | 0.43 | 4.50 |

## Conclusions

We have prepared and fully characterized 6-(1-methyl-1*H*-pyrrol-2-yl)-2,2′-bipyridine, **3**, and 6-(selenophene-2-yl)-2,2′-bipyridine, **4**. Copper(I) complexes $[CuL_2][PF_6]$ in which L is 2,2′-bipyridine substituted in the 6-position by methyl, phenyl or an aromatic heterocyclic substituent (L = **1–6**) have been synthesized. These have been characterized by electrospray mass spectrometry, solution NMR and electronic absorption spectroscopies, and, for $[Cu(\mathbf{1})_2][PF_6]$, $[Cu(\mathbf{2})_2][PF_6]$, $[Cu(\mathbf{3})_2][PF_6]$, $[Cu(\mathbf{5})_2][PF_6]$ and $[Cu(\mathbf{6})_2][PF_6]$, single crystal X-ray diffraction structure determinations. In each of $[Cu(\mathbf{1})_2][PF_6]$, $[Cu(\mathbf{2})_2][PF_6]$, $[Cu(\mathbf{3})_2][PF_6]$ and $[Cu(\mathbf{5})_2][PF_6]$, the heterocyclic or phenyl substituent is twisted out of the plane of the bpy unit. In $[Cu(\mathbf{3})_2][PF_6]$ and $[Cu(\mathbf{5})_2][PF_6]$, this results in inter-ligand π-stacking which is particularly efficient in the former, despite the presence of the *N*-methyl substituents. In $[Cu(\mathbf{2})_2][PF_6]$, inter-ligand face-to-face stacking is achieved by a combination of substituent twisting and elongation of one Cu–N bond. In contrast, no intra-cation π-stacking between ligands is observed in $[Cu(\mathbf{1})_2][PF_6]$. The copper(I) ion in $[Cu(\mathbf{6})_2][PF_6]$ is in an approximately tetrahedral coordination environment.

Complexes $[CuL_2][PF_6]$ (L = **1–6**) undergo ligand exchange reactions with $TiO_2$-anchored ligands **7–10** (L′) to generate a

series of 24 surface-anchored heteroleptic copper(I) complexes. MALDI-TOF mass spectrometry and diffuse reflectance UV-VIS spectroscopy have been used to provide evidence of the formation of the latter, and their efficiencies as dyes in DSCs have been screened. The greatest efficiencies were observed for [CuLL′] in which L′ = **10** which contains phosphonate anchoring groups.

## Acknowledgements

We thank the Swiss National Science Foundation, the European Research Council (Advanced Grant 267816 LiLo) and the University of Basel for financial support. $^{77}$Se NMR spectra were recorded by PD Dr Daniel Häussinger. Michael Liebetanz is thanked for growing crystals of [Cu(**1**)$_2$][$PF_6$].

## Notes and references

1 T. Bessho, E. C. Constable, M. Grätzel, A. Hernandez Redondo, C. E. Housecroft, W. Kylberg, Md. K. Nazeeruddin, M. Neuburger and S. Schaffner, *Chem. Commun.*, 2008, 3717.
2 N. Alonso-Vante, V. Ern, P. Chartier, C. O. Dietrich-Buchecker, D. R. McMillin, P. A. Marnot and J.-P. Sauvage, *Nouv. J. Chim.*, 1983, 3.
3 N. Alonso-Vante, J.-F. Nierengarten and J.-P. Sauvage, *J. Chem. Soc., Dalton Trans.*, 1994, 1649.
4 E. C. Constable, A. Hernandez Redondo, C. E. Housecroft, M. Neuburger and S. Schaffner, *Dalton Trans.*, 2009, 6634.
5 S. Sakati, T. Kuroki and T. Hamada, *J. Chem. Soc., Dalton Trans.*, 2002, 840.
6 A. Hernandez Redondo, E. C. Constable and C. E. Housecroft, *Chimia*, 2009, **63**, 205.
7 C. L. Linfoot, P. Richardson, T. E. Hewat, O. Moudam, M. M. Forde, A. Collins, F. White and N. Robertson, *Dalton Trans.*, 2010, **39**, 8945.
8 K. H. Kim, T. Okubo, N. Tanaka, N. Mimura, M. Maekawa and T. Kuroda-Sowa, *Chem. Lett.*, 2010, **39**, 792.
9 B. Bozic-Weber, E. C. Constable, C. E. Housecroft, M. Neuburger and J. R. Price, *Dalton Trans.*, 2010, **39**, 3585.
10 E. C. Constable, C. E. Housecroft, M. Neuburger, J. Price, A. Wolf and J. A. Zampese, *Inorg. Chem. Commun.*, 2010, **13**, 74.
11 D. V. Scaltrito, D. W. Thompson, J. A. O'Callaghan and G. J. Meyer, *Coord. Chem. Rev.*, 2000, **208**, 243.
12 Y. Jahng, J. Hazelrigg, D. Kimball, E. Riesgo, R. Wu and R. P. Thummel, *Inorg. Chem.*, 1997, **36**, 5390.
13 J. R. Nitschke, *Angew. Chem., Int. Ed.*, 2004, **43**, 3073.
14 D. Schultz and J. R. Nitschke, *J. Am. Chem. Soc.*, 2006, **128**, 9887.
15 R. J. Sarma and J. R. Nitschke, *Angew. Chem., Int. Ed.*, 2008, **47**, 377.
16 M. T. Miller, P. K. Gantzel and T. B. Karpishin, *J. Am. Chem. Soc.*, 1999, **121**, 4292.
17 E. C. Constable, C. E. Housecroft, P. Kopecky, E. Schönhofer and J. A. Zampese, *CrystEngComm*, 2011, **13**, 2742.
18 J. Schönle, *M.Sc. Thesis*, University of Basel, 2010.
19 N. Armaroli, G. Accorsi, F. Cardinali and A. Listorti, *Top. Curr. Chem.*, 2007, **280**, 69.
20 H. J. Bolink, E. Coronado, R. D. Costa, E. Ortí, M. Sessolo, S. Graber, K. Doyle, M. Neuburger, C. E. Housecroft and E. C. Constable, *Adv. Mater.*, 2008, **20**, 3910; S. Graber, K. Doyle, M. Neuburger, C. E. Housecroft, E. C. Constable, R. D. Costa, E. Ortí and H. J. Bolink, *J. Am. Chem. Soc.*, 2008, **130**, 14944; H. J. Bolink, E. C. Constable, E. Coronado, R. D. Costa, S. Graber, C. E. Housecroft, N. Lardiés, M. Neuburger, E. Ortí, S. Schaffner and M. Sessolo, *Chem. Commun.*, 2009, 2029; H. J. Bolink, E. Coronado, R. D. Costa, N. Lardiés, E. Ortí, S. Graber, M. Neuburger, C. E. Housecroft, S. Schaffner and E. C. Constable, *Adv. Funct. Mater.*, 2009, **19**, 3456; R. D. Costa, H. J. Bolink, E. Ortí, M. Sessolo, S. Graber, K. Doyle, M. Neuburger, C. E. Housecroft and E. C. Constable, *Mater. Res. Soc. Symp. Proc.*, 2009, **1114**, 1114-G12-19; R. D. Costa, E. Ortí, H. J. Bolink, S. Graber, C. E. Housecroft and E. C. Constable;, *Adv. Funct. Mater.*, 2010, **20**, 1511; R. D. Costa, E. Ortí, H. J. Bolink, S. Graber, C. E. Housecroft and E. C. Constable, *J. Am. Chem. Soc.*, 2010, **132**, 5978; R. D. Costa, E. Ortí, H. J. Bolink, S. Graber, C. E. Housecroft and E. C. Constable, *Chem. Commun.*, 2011, **47**, 3207; R. D. Costa, E. Ortí, D. Tordera, A. Pertegás, H. J. Bolink, S. Graber, C. E. Housecroft, L. Sachno, M. Neuburger and E. C. Constable, *Adv. Energy Mater.*, 2011, **1**, 282.
21 See for example: C. T. Cunningham, K. L. H. Cunningham, J. F. Michalec and D. R. McMillin, *Inorg. Chem.*, 1999, **38**, 4388; C. T. Cunningham, J. J. Moore, K. L. H. Cunningham, P. E. Fanwick and D. R. McMillin, *Inorg. Chem.*, 2000, **39**, 3638 and references therein.
22 See for example: R. O. Steen, L. J. Nurkkala, S. J. Angus-Dunne, C. X. Schmitt, E. C. Constable, M. J. Riley, P. V. Bernhardt and S. J. Dunne, *Eur. J. Inorg. Chem.*, 2008, 1784; L. J. Nurkkala, R. O. Steen, H. K. J. Friberg, J. A. Häggström, P. V. Bernhardt, M. J. Riley and S. J. Dunne, *Eur. J. Inorg. Chem.*, 2008, 4101; I. H. Jenkins, N. G. Rees and P. G. Pickup, *Chem. Mater.*, 1997, **9**, 1213.
23 E. C. Constable, P. R. G. Henney and T. A. Leese, *J. Organomet. Chem.*, 1989, **361**, 277.
24 E. C. Constable, R. P. G. Henney, P. R. Raithby and L. R. Sousa, *Angew. Chem., Int. Ed. Engl.*, 1991, **30**, 1363.
25 W. Lu, N. Zhu and C.-M. Che, *Chem. Commun.*, 2002, 900.
26 W. Lu, M. C. W. Chan, N. Zhu, C.-M. Che, C. Li and Z. Hui, *J. Am. Chem. Soc.*, 2004, **126**, 7639.
27 E. C. Constable, R. P. G. Henney and D. A. Tocher, *J. Chem. Soc., Chem. Commun.*, 1989, 913.
28 E. C. Constable, R. P. G. Henney and D. A. Tocher, *J. Chem. Soc., Dalton Trans.*, 1991, 2335.
29 E. C. Constable, R. P. G. Henney, P. R. Raithby and L. R. Sousa, *J. Chem. Soc., Dalton Trans.*, 1992, 2251.
30 G. R. Haire, N. E. Leadbeater, J. Lewis, P. R. Raithby, A. J. Edwards and E. C. Constable, *J. Chem. Soc., Dalton Trans.*, 1997, 2997.
31 F. Kröhnke, *Synthesis*, 1976, 1.
32 J.-K. Son, L.-X. Zhao, A. Basnet, P. Thapa, R. Karki, Y. Na, Y. Jahng, T. C. Jeong, B.-S. Jeong, C.-S. Lee and E.-S. Lee, *Eur. J. Med. Chem.*, 2008, **43**, 675.
33 G. J. Kubas, *Inorg. Synth.*, 1990, **28**, 68.
34 C. O. Dietrich-Buchecker, P. A. Marnot and J.-P. Sauvage, *Tetrahedron Lett.*, 1982, **23**, 5291.
35 R. O. Steen, L. J. Nurkkala, S. J. Angus-Dunne, C. X. Schmitt, E. C. Constable, M. J. Riley, P. V. Bernhardt and S. J. Dunne, *Eur. J. Inorg. Chem.*, 2008, 1784.
36 D. L. Jameson and L. E. Guise, *Tetrahedron Lett.*, 1991, **32**, 1999.
37 A.-K. Pleier, H. Glas, M. Grosche, P. Sirsch and W. R. Thiel, *Synthesis*, 2001, **1**, 55.
38 F. A. Rosa, P. Machado, H. G. Bonacorso, N. Zanatta and M. A. P. Martins, *J. Heterocycl. Chem.*, 2008, **45**, 879.
39 J.-K. Son, L.-X. Zhao, A. Basnet, P. Thapa, R. Karki, Y. N. Y. Jahng, T. C. Jeong, B-S Jeong, C-S Lee and E.-S. Lee, *Eur. J. Med. Chem.*, 2008, **43**, 675.
40 *Bruker* Analytical X-ray Systems Inc, 2006, APEX2, version 2 User Manual, M86-E01078, Madison, WI.
41 A. Altomare, G. Cascarano, G. Giacovazzo, A. Guagliardi, M. C. Burla, G. Polidori and M. Camalli, *J. Appl. Crystallogr.*, 1994, **27**, 435.
42 P. W. Betteridge, J. R. Carruthers, R. I. Cooper, K. Prout and D. J. Watkin, *J. Appl. Crystallogr.*, 2003, **36**, 1487.
43 Stoe & Cie, *IPDS* software v 1.26, Stoe & Cie, Darmstadt, Germany, 1996.
44 G. M. Sheldrick, *Acta Crystallogr., Sect. A: Found. Crystallogr.*, 2008, **64**, 112.
45 L. J. Farrugia, *J. Appl. Crystallogr.*, 1997, **30**, 565.
46 I. J. Bruno, J. C. Cole, P. R. Edgington, M. K. Kessler, C. F. Macrae, P. McCabe, J. Pearson and R. Taylor, *Acta Crystallogr., Sect. B: Struct. Sci.*, 2002, **58**, 389.
47 C. F. Macrae, I. J. Bruno, J. A. Chisholm, P. R. Edgington, P. McCabe, E. Pidcock, L. Rodriguez-Monge, R. Taylor, J. van de Streek and P. A. Wood, *J. Appl. Crystallogr.*, 2008, **41**, 466.
48 J. G. Park and Y. Jahng, *Bull. Korean Chem. Soc.*, 1998, **19**, 436.
49 E. Jones and I. M. Moodie, *Org. Synth.*, 1970, **50**, 104.
50 T. Nagata and K. Tanaka, *Bull. Chem. Soc. Jpn.*, 2002, **75**, 2469.
51 C. Thone, F. Vancea and P. G. Jones, private communication to the Cambridge Structural Database, 2010, refcodes QUWDES, QUWDUI.
52 D. Das, G. K. Rao and A. K. Singh, *Organometallics*, 2009, **28**, 6054.
53 P. Péchy, F. P. Rotzinger, Md. K. Nazeeruddin, O. Kohle, S. M. Zakeeruddin, R. Humphry-Baker and M. Grätzel, *J. Chem. Soc., Chem. Commun.*, 1995, 65.
54 A. Hernández Redondo, Ph.D. Thesis, University of Basel, 2009.



 